Ethylene/Norbornene Copolymerizations with Titanium CpA Catalysts

Andrew L. McKnight and Robert M. Waymouth*

Department of Chemistry, Stanford University, Stanford, California 94305

Received August 28, 1998; Revised Manuscript Received March 2, 1999

ABSTRACT: Group 4 *ansa*-cyclopentadienylamido (CpA) complexes $[Me_2Si(Cp')(NR)]MCl_2$ (R = alkyl, M = Ti, Zr) efficiently copolymerize ethylene with a variety of α-olefins. Ethylene/norbornene copolymerization reactivity ratios were determined at 40 °C for CpA catalysts $[Me_2Si(Cp')(N^tBu)]TiCl_2$ (Cp′ = Me_4Cp, 2,4-Me_2Cp, 3-^{t}BuCp, Ind), and the resulting values are low ($r_1 = 2.0-5.1$, $r_2 \rightarrow 0$), suggesting a tendency toward alternating comonomer insertion at high norbornene/ethylene feed ratios. As reaction temperature is increased and norbornene concentration is decreased, productivity increases and norbornene incorporation decreases. No more than 46 mol % norbornene is incorporated into the copolymer using these CpA catalysts even at low feed ratios (E/N ≥ 0.02), and norbornene homopolymerizations with $[Me_2Si(Me_4Cp)(N^tBu)]TiCl_2$ proceed to very low conversion (<1%). ^{13}C NMR spectroscopy of CpA-derived poly(ethylene-*co*-norbornene)s shows the copolymers contain virtually no consecutive norbornene sequences, and the microstructure of the resulting ethylene norbornene copolymers is dependent on catalyst geometry.

Monocyclopentadienylamido (CpA)−titanium complexes are an interesting class of polymerization catalysts due to their ability to copolymerize ethylene with olefins such as octene[1−4] and styrene.[4−6] The combination of the CpA catalysts' ability to produce high molecular weight, low-density polyolefins at high reactor temperatures has led to rapid commercialization of this catalyst technology.[7,8]

Our investigations into propylene homopolymerizations with CpA catalysts revealed low stereospecificity, presumably as a consequence of the sterically unencumbered active site coupled with a relatively small monomer. For propylene polymerizations stereospecificity is extremely low and is largely unaffected by changes in catalyst structure.[9] CpA titanium catalysts that have tetramethylcyclopentadienyl or indenyl rings also give rise to significant regioirregularities in the polypropylene chain. As a result, we were interested in exploring polymerization systems where catalyst site control might be possible.

One type of monomer that would be expected to more directly interact with the CpA catalyst structure is bulky cyclic olefins such as norbornene. The addition polymerization of hindered cyclic olefins such as cyclopentene, cyclohexene, and norbornene without significant ring opening polymerization has proven to be difficult for traditional heterogeneous Ziegler−Natta catalysts.[10] Addition polymerization of norbornene was first described in the 1960s with homogeneous palladium(II) catalysts,[11] and these catalysts have been further investigated by Sen[12] and Risse.[13] The ensuing years have witnessed advances by Kaminsky[14−17] and Goodall,[18] who reported the use of zirconocenes and cobalt salts for the preparation of poly(norbornene) and poly(ethylene-*co*-norbornene). The addition homopolymers and copolymers of norbornene constitute an important set of materials because of their high glass transition temperatures and improved heat resistance over polyethylene.[19]

At the onset of our studies, the ability of CpA catalysts to copolymerize bulky olefins such as norbornene with ethylene received only scattered attention in the patent literature,[3,5,20−24] and a general understanding of their inherent reactivities in this copolymerization system was not known. Given the great interest in norbornene homo- and copolymers, and the possibility that the CpA catalysts might exhibit different selectivities than other catalyst systems, we conducted a systematic study of the CpA ethylene/norbornene copolymerization system. As these studies were being completed, Fink and coworkers reported a detailed study of the copolymerization of ethylene and norbornene with several metallocene and CpA catalysts,[25−28] and Harrington reported a stereoregular alternating EN copolymer.[24] In this paper we present the results of these studies with specific regard to the effects of the cyclopentadienyl fragment on monomer reactivity ratios and copolymer microstructure.

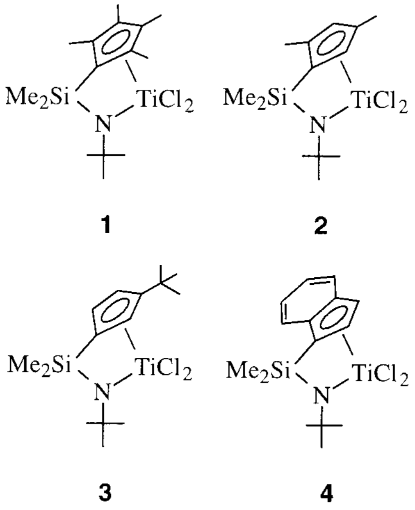

Figure 1. C_s and C_1 symmetric CpA catalysts for copolymerizations.

Results

Catalyst Synthesis. Shown in Figure 1 are four CpA catalysts we targeted to probe the influence of catalyst symmetry and structure on norbornene incorporation and copolymer microstructure. The synthesis of these

10.1021/ma981365v CCC: $18.00

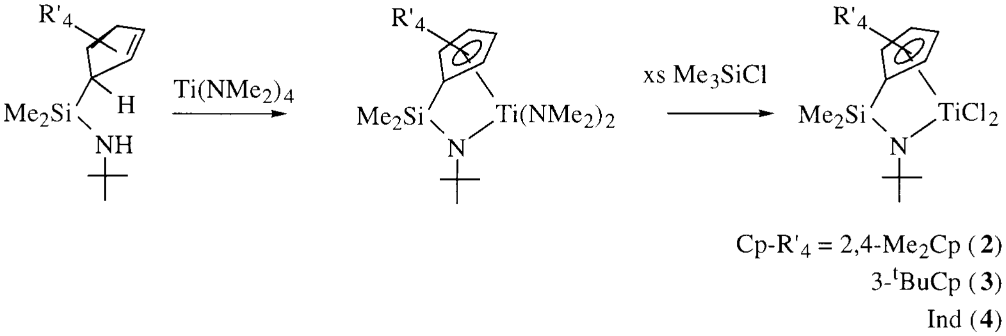

Figure 2. Amine elimination synthesis of CpA complexes.

Table 1. Norbornene Homopolymerizations with Zirconocene and CpA Catalysts[a]

expt	catalyst	*T* (°C)	yield (g)	product. (kg/mol M mol N)
1	**1**	22	0.042	187
2	**5**	22	0.167	742
3	**6**	22	0.020	88
4	**1**	80	0.115	511

[a] Conditions: [cat] = 20 mM, Al/M = 2000 (M = Ti, Zr), [N] = 4.50 M, solvent = toluene, *V* = 50 mL, *t* = 8 days.

complexes was accomplished by two different methods: one a standard salt metathesis route and the other an amine elimination route.[29–31] Complex **1** was prepared by converting the neutral ligand to the dimagnesiochloride salt and then reacting with $TiCl_3(THF)_3$ with a subsequent $PbCl_2$ oxidation.[9,32] In the second approach, reaction of a neutral Cp–amide ligand and $Ti(NMe_2)_4$ in refluxing toluene over several days led to complete production of the ligated bis(dimethylamido)titanium complex. The bis(dimethylamide) can be converted cleanly to the dichloride by treatment with excess Me_3SiCl in methylene chloride (Figure 2).[30,31] This method gives moderate to high yields (30–70%) of titanium complexes **2**, **3**, and **4**, but no conversion is observed when Cp–R′$_4$ = Me_4Cp, presumably due to the steric demands of this ligand.

Norbornene Homopolymerization. Homopolymerizations of norbornene were carried out with $[Me_2Si(Me_4Cp)(N^tBu)]TiCl_2$ (**1**) and with the two zirconocenes *rac*-$[Et(Ind)_2]ZrCl_2$ (**5**) and $[Me_2C(Flu)(Cp]ZrCl_2$ (**6**) under high norbornene concentration at extended reaction times in order to isolate measurable yields of polymer. Table 1 lists the results of these experiments, which show that at 22 °C all three catalysts are poor norbornene polymerization catalysts. Of the three catalysts, C_2-symmetric *rac*-$[Et(Ind)_2]ZrCl_2$ (**5**) exhibited the highest productivity, followed by **1** and then **6**. The results for **5** and **6** also suggest that an earlier assertion that C_s-symmetric catalysts are more active than C_2-symmetric catalysts[16] depends on the catalyst system; in that particular case, *rac*-[$\mathbf{R_2Si}$(Ind)$_2$]$ZrCl_2$ (R = Me, Ph) catalysts were investigated. Our results for catalyst **1** also show that homopolymerization productivity can be increased by a factor of 6 when the reaction temperature is increased to 80 °C.

Ethylene/Norbornene Copolymerizations. Copolymerizations of ethylene and norbornene were carried out with catalysts **1**–**6** and MAO over several feed ratios at 40 °C. Reaction times were varied to keep conversion low (10–15%) while yielding enough copolymer to be produced for subsequent characterizations by NMR, GPC, and DSC. Data for selected copolymerizations are listed in Table 2.

Productivities normalized to the total olefin concentration are listed in Table 2. The data show that as the feed ratio (=[E]/[N]) decreases from 2.57 to 0.05 in copolymerizations with $[Me_2Si(Me_4Cp)(N^tBu)]TiCl_2$ (**1**), productivities decrease accordingly. Generally **1** is the most productive CpA catalyst;[26] analogous copolymerizations with $[Me_2Si(Me_2Cp)(N^tBu)]TiCl_2$ (**2**) and $[Me_2Si(Ind)(N^tBu)]TiCl_2$ (**4**) are approximately 3–10 times less productive, as are comparative copolymerizations with $[Me_2Si(3\text{-}^tBuCp)(N^tBu)]TiCl_2$ (**3**) (4000 g/mmol·h·M for E/N = 0.43/1.09 and 2600 g/mmol·h·M for E/N = 0.32/1.09). CpA catalyst **1** is also more productive than the two zirconocene catalysts *rac*-$[Et(Ind)_2]ZrCl_2$ (**5**) and $[Me_2C(Flu)(Cp)]ZrCl_2$ (**6**) under similar conditions.

As expected, norbornene incorporation for **1** is inversely dependent on the E/N feed ratio, and a low ratio (=0.05) is needed to produce a copolymer containing 46% norbornene for this catalyst. In general, the CpA and zirconocene catalysts listed in Table 2 incorporate norbornene with similar efficiencies at similar feed ratios. Only the *tert*-butyl catalyst **3** requires a low feed ratio (=0.05) to incorporate 34% norbornene.

The current interest in P(E-*co*-N)s is derived from the high glass transition temperatures (T_g) and high melting points (T_m) of some of the copolymers. As more norbornene is incorporated into copolymers derived from **1**, T_g's increase as expected up to values as high as 130 °C. The glass transition temperatures reported in Table 2 fall within the range of values reported for P(E-*co*-N)'s of similar compositions.[15–17,19,33,34] The nature of the catalyst precursor appears to have little effect on T_g (for this series of catalysts) as copolymers with 34 mol % N made from six different catalysts have T_g values between 67 and 84 °C.

Harrington and Crowther recently reported[22,24] that chiral hafnium and zirconium CpA catalysts of the same symmetry as **3** are able to produce semicrystalline P(E-*co*-N)s with remarkably high melting points (250 °C). It was suggested that the crystallinity was due to an alternating and stereospecific comonomer distribution in the polymer chain. To date we have not observed any high melting transitions for any of the copolymers of this study, particularly for high norbornene content (>35%) annealed P(E-*co*-N) samples 5, 6, 8, or 9 in heating scans from 25 to 350 °C.

Determination of the molecular weights of P(E-*co*-N)s is complicated by low d*n*/d*c* values for the copolymers, and thus refractive index detection does not show a significant response. Table 2 lists the results of two types of detection methods: refractive index and viscometry. Only selected data were obtained using DRI detection, due to compositional sensitivity. As Bergström reported previously,[35] the polarity of the RI signal

Table 2. Ethylene/Norbornene Copolymerizations Using Catalysts 1−6[a]

entry	cat[b]	P(E)[c] (bar)	[E] (M)	[N] (M)	product.[d] (g/mmol h M)	incorp[e] (mol %)	T_g[f] (°C)	DRI[g] M_w ($\times10^{-3}$)	DRI[g] PDI	viscometry[h] M_w ($\times10^{-3}$)	viscometry[h] PDI
1	**1**	4.9	0.54	0.21	28000	11.7	34.8	64	3.8	164	2.1
2	**1**	4.9	0.54	0.54	31400	22.0	n.d.	174	2.6	341	1.8
3	**1**	3.9	0.43	1.09	10500	30.1	59.9	548	2.5	1190	1.8
4	**1**	2.9	0.32	1.09	6810	34.3	76.4			360	1.7
5	**1**	2.9	0.32	2.19	4780	40.3	94.1	564	2.2	862	1.7
6	**1**	0.9	0.10	2.19	480	46.3	127.1	285	2.2	390	1.7
7	**2**	4.9	0.54	1.09	2880	34.0	67.2	353	2.2	401	1.7
8	**3**	0.9	0.10	1.09	437	35.1	70.9			253	1.7
9	**4**	3.9	0.43	1.09	921	34.5	83.5			396	1.8
10	**5**	4.9	0.54	0.54	22000	34.7	76.5				
11	**6**	2.9	0.32	1.09	2550	34.4	76.2	178	1.7	225	1.7

[a] Conditions: [cat] = 20 μmol, Al/M = 2000, T = 40 °C, solvent = toluene. [b] **1** = $[Me_2Si(Me_4Cp)(N^tBu)]TiCl_2$, **2** = $[Me_2Si(2,4\text{-}Me_2Cp)(N^tBu)]TiCl_2$, **3** = $[Me_2Si(3\text{-}^tBuCp)(N^tBu)]TiCl_2$, **4** = $[Me_2Si(Ind)(N^tBu)]TiCl_2$, **5** = *rac*-$[Et(Ind)_2]ZrCl_2$, **6** = $[Me_2C(Flu)(Cp)]ZrCl_2$. [c] Ethylene pressure corrected for nitrogen in the reactor. [d] Productivity in g P(E-*co*-N)/mmol metal h ([E] + [N]). [e] Norbornene incorporation, by ^{13}C NMR. [f] By DSC. [g] GPC molecular weights and polydispersities versus polystyrene by differential refractive index. [h] GPC molecular weights and polydispersities versus polystyrene by viscometry.

Table 3. E/N Reactivity Ratios for CpA Catalysts

catalyst	r_1	r_2
$[Me_2Si(Me_4Cp)(N^tBu)]TiCl_2$ (**1**)	2.4	∼0
$[Me_2Si(2,4\text{-}Me_2Cp)(N^tBu)]TiCl_2$ (**2**)	1.9	∼0
$[Me_2Si(3\text{-}^tBuCp)(NtBu)]TiCl_2$ (**3**)	5.1	∼0
$[Me_2Si(Ind)(N^tBu)]TiCl_2$ (**4**)	2.2	∼0

reverses at high norbornene contents, and samples with approximately 34% norbornene show no signal. The RI and viscometry data, however, show that copolymers produced by CpA catalysts generally have high molecular weights and narrow molecular weight distributions.[28] The anomalously high molecular weights for P(E-*co*-N) samples 3 and 5 may be the result of unusual viscosities for these compositions. Although the data in Table 2 do not suggest any trends in norbornene effects on molecular weight, Fink noted that catalyst **1** surprisingly gives copolymers of decreasing molecular weight with increasing norbornene content.[28] This is opposite the behavior observed for metallocene catalysts and could be attributed to chain transfer from the M−E* active site facilitated by a penultimate norbornene unit. And while metallocene catalysts of the structure $[Me_2C(Flu)(3\text{-}R{-}Cp)]ZrCl_2$ (R = H, Me, ^{i}Pr, ^{t}Bu) show increased molecular weight with increased ligand bulk,[28] the steric nature of the CpA ligand does not have a clear effect on the resulting copolymer molecular weights (entries 4, 7, 8, and 9).

Determination of Ethylene/Norbornene Reactivity Ratios for CpA Catalysts. To calculate the ethylene/norbornene reactivity ratios for the CpA catalysts of this study according to the Fineman−Ross method, several copolymerizations of ethylene and norbornene were carried out with catalysts **1**−**4** and MAO over a broad range of monomer ratios at 40 °C. Data for these copolymerizations and the Fineman−Ross plots are listed in the Supporting Information, and the results of the reactivity ratio calculations are shown in Table 3. Catalysts **1**, **2**, and **4** give r_1 values near 2.0, while catalyst **3** has an r_1 value of 5.1, presumably because it is the most sterically encumbered of the four CpA catalysts. The low r_1 values are consistent with values for ethylene/octene copolymerizations (r_1 = 2.6−4) with CpA catalysts[36,37] and indicate a preference for insertion of ethylene over norbornene into a M−E* active center. In all cases, the intercepts were very close to zero, and as a result it was not possible to accurately determine r_2 from the plots. However, the data are consistent with an r_2 very close to zero given the low norbornene homopolymerization productivities for **1**.

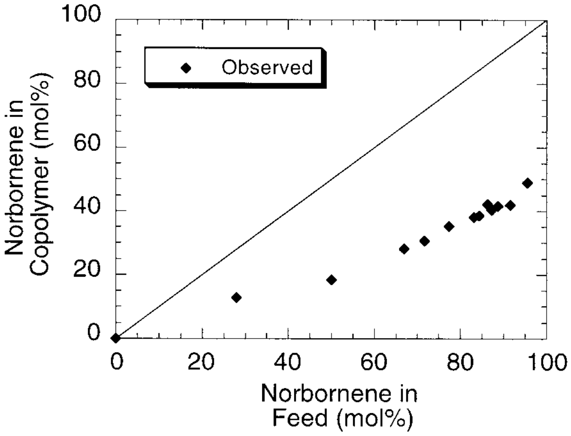

Figure 3. Dependence of the instantaneous copolymer composition on the initial monomer feed composition for ethylene/norbornene copolymerizations with **1**/MAO.

The copolymerization diagram in Figure 3 illustrates the linear relationship for ideal systems (r_1r_2 = 1), superimposed by data for poly(ethylene-*co*-norbornene)s produced by $[Me_2Si(Me_4Cp)(N^tBu)]TiCl_2$ (**1**). The product of the reactivity ratios for the CpA ethylene/norbornene system approaches zero, indicating a tendency away from ideal behavior and toward alternation. This tendency toward alternation is reflected by the observation that even at very high norbornene to ethylene feed ratios it is difficult for **1** to incorporate more than 50 mol % norbornene in the copolymer. In fact, an N/E mole ratio of 22 was necessary to obtain 46 mol % N in a copolymer produced by **1**. In contrast, some metallocene catalysts[27,38] are known to incorporate greater than 50 mol % norbornene and other polycyclic olefins at high norbornene feed concentrations (>80 mol %).

Determination of E/N Reactivity Ratios for Zirconocenes. Kaminsky and Fink have investigated the activity of various zirconocenes in homo- and copolymerizations of strained cyclic olefins with ethylene.[15−17,27,38−43] To relate the polymerization behavior of CpA catalysts to zirconocenes, three typical zirconium catalysts of different symmetries shown in Figure 4 were selected for comparative copolymerization studies. The first catalyst chosen was the C_2-symmetric *rac*-ethylenebis(indenyl)zirconium dichloride, (*rac*-$[Et(Ind)_2]ZrCl_2$, **5**), which is a known[44] isospecific α-olefin polymerization catalyst and was reported by Berg-

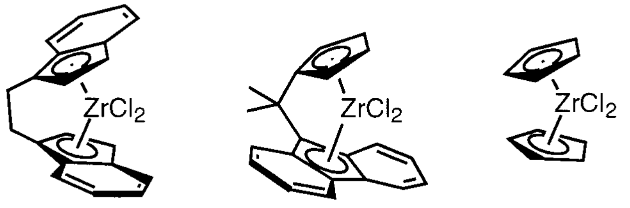

5 **6** **7**

Figure 4. Bridged and unbridged zirconocenes for comparative copolymerizations.

Table 4. E/N Reactivity Ratios for Zirconocene Catalysts

catalyst	r_1	r_2
rac-$[Et(Ind)_2]ZrCl_2$ (**5**)	1.9	0.03
$[Me_2C(Flu)(Cp)]ZrCl_2$ (**6**)	1.8	~0
Cp_2ZrCl_2 (**7**)	4.0	0.03

Table 5. Temperature Effects in Ethylene/Norbornene Copolymerizations with $[Me_2Si(Me_4Cp)(N^tBu)]TiCl_2$ (1)[a]

entry	press.[b] (bar)	[E] (M)	*T* (°C)	yield (g)	product. kg/(mol h)	incorp[c] (mol %)
13	1.3	0.14	40	1.650	6600	41.2
14	1.6	0.14	60	2.220	8880	39.6
15	2.1	0.14	80	3.330	13320	37.7

[a] Conditions: [**1**] = 20 μM, Al/Ti = 2000, V = 50 mL, t = 15 min, [N] = 1.09 M, solvent = toluene. [b] Ethylene pressure corrected for nitrogen in reactor. [c] Norbornene incorporation, determined by ^{13}C NMR.

Table 6. Reported Reactivity Ratios for Zirconocene Catalysts in Ethylene/Norbornene Copolymerizations

catalyst	r_1	r_2	*T* (°C)	ref
rac-$[Et(Ind)_2]ZrCl_2$ (**5**)	6.6	–	25	15
	1.9	0.03	40	*a*
rac-$[Et(Ind\text{-}H_4)_2]ZrCl_2$	2.2, 3.3	–, –	25, 50	15
rac-$[Me_2Si(Ind)_2]ZrCl_2$	3.69, 2.66	–, 0.36	25, 30	16, 53
rac-$[Ph_2Si(Ind)_2]ZrCl_2$	3.44	–	30	16
$[Me_2C(Ind)(Cp)]ZrCl_2$	0.88	0.05	70	27
$[Me_2C(Ind)(3\text{-}MeCp)]ZrCl_2$	1.14	0.10	70	27
$[Me_2C(Ind)(3\text{-}^tBuCp)]ZrCl_2$	1.1	0.026	70	27
$[Me_2C(Flu)(Cp)]ZrCl_2$ (**6**)	2.93	–	30	16
	1.8	~0	40	*a*
	1.3	0.03	70	27
$[Ph_2C(Flu)(Cp)]ZrCl_2$	1.85, 2.61	–	0, 30	16
$[Me_2C(Flu)(3\text{-}MeCp)]ZrCl_2$	$r_{11} = 1.2$, $r_{21} = 3.6$	–	70	27
$[Me_2C(Flu)(3\text{-}^iPrCp)]ZrCl_2$	4.15	0.033	30	17
	$r_{11} = 2.2$, $r_{21} = 2.7$	–	70	27
$[Me_2Si(Flu)(3\text{-}^tBuCp)]ZrCl_2$	$r_{11} = 5.2$, $r_{21} = 18.2$	–	70	27
$[Me_2C(Flu)(3\text{-}^tBuCp)]ZrCl_2$	3.05	–	30	17
	$r_{11} = 2.2$, $r_{21} = 8.9$	–	70	27
$[MeCH(Cp)_2]ZrCl_2$	0.83	0.29	70	27
Cp_2ZrCl_2 (**7**)	20	–	25	15
	4.0	0.03	40	*a*

[a] This work.

ström[33] to give significant levels (10%) of norbornene block sequences in poly(ethylene-*co*-norbornene). The other zirconocene investigated was $[Me_2C(Flu)(Cp)]ZrCl_2$ (**6**), which is known to be a syndiospecific α-olefin polymerization catalyst due to its C_s symmetry.[45,46] Kaminsky found both catalysts to be very active in ethylene–norbornene copolymerizations.[16,17] Finally, the unbridged, achiral zirconocene Cp_2ZrCl_2 (**7**) was selected because it was found to show a lower preference for norbornene in copolymerization reactions.[15]

To calculate the ethylene/norbornene reactivity ratios for these zirconocenes according to the Fineman–Ross method, several copolymerizations of ethylene and norbornene were carried out with catalysts **5**–**7** and MAO over a broad range of monomer ratios at 40 °C. Data for these copolymerizations and the Fineman–Ross plots are listed in the Supporting Information, and the results of the reactivity ratio calculations are shown in Table 4.

Bridged zirconocenes **5** and **6** have r_1 values near 2.0 similar to the CpA catalysts **1**, **2**, and **4**. Catalyst **7** has an r_1 value of 4.0, reflecting the steric influence of the unbridged cyclopentadienyl rings. The r_1 values for all three catalysts indicate a preference for insertion of ethylene over norbornene into an active M–E* center but under our conditions are lower than those previously reported.[15,17]

From the Fineman–Ross plots for **5** and **7** we were able to calculate r_2 values of 0.03, while the plot for **6** indicated its r_2 value was very close to zero. This clearly illustrates that these catalysts also discourage norbornene homopropagation because of the steric influence of the last inserted norbornene unit. Like the CpA catalysts, these zirconococenes should have a tendency to produce alternating microstructures at high norbornene to ethylene feed ratios.[26]

Temperature Effects. We initially chose to conduct all copolymerizations at 40 °C to allow comparison with reactivity ratios and productivities of the ethylene/styrene copolymerization system studied by Sernetz, who found $r_1 = 23.4$ and $r_2 = 0.015$ for $[Me_2Si(Me_4Cp)(N^tBu)]TiCl_2$ (**1**).[6] As catalyst productivity and the relative rate of norbornene incorporation would be expected to be temperature dependent, copolymerizations were carried out at 40, 60, and 80 °C using catalyst **1** at constant monomer concentrations. The results summarized in Table 5 show there is a nonlinear dependence of productivity on temperature over the temperature range investigated. As the reaction temperature is increased, norbornene incorporation drops off slightly, and so does the relative ratio of the C_1 methynes at 47.9 and 47.3 ppm (vide infra). Such behavior is often[15,16,42] attributed to an increase in r_1 and a decrease in r_2 with increasing temperature.

Discussion

Catalyst Reactivity. All of the CpA catalysts, with the exception of $[Me_2Si(3\text{-}^tBuCp)(N^tBu)]TiCl_2$ (**3**), have r_1 values around 2.0 and r_2 values very close to zero, indicating a preference for ethylene insertion over multiple norbornene insertion. Fineman–Ross plots are limited in their ability to accurately calculate r_2, since in many cases there is an uneven distribution of experimental composition data. However, analysis by the Kelen–Tüdos method[47] gives similar results for r_1 and r_2, with the latter being very close to zero. Zirconocenes **5** and **6** exhibited similar copolymerization behavior, but the calculated r_1 values (1.9 and 1.8, respectively) were lower than those previously reported (Table 6).[15,16] The r_1 value of 4.0 for **7** is also lower than the literature value. This discrepancy might be attributed to the different reaction temperatures.

Catalyst **3**, with a bulky *tert*-butyl group in the cyclopentadienyl β-position, has the largest r_1 value (=5.1), reflecting the influence of nonbonding interactions between the ligand and the large cyclic olefin. In general, all of the CpA catalysts are able to efficiently incorporate 30–40% of norbornene into a polyethylene backbone. However, we have been unable to incorporate

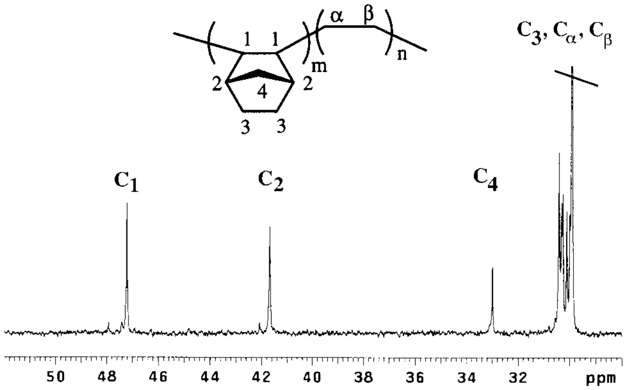

Figure 5. Structure, numbering scheme, and literature ^{13}C NMR assignments for poly(ethylene-*co*-norbornene). The spectrum shown is for entry 2.

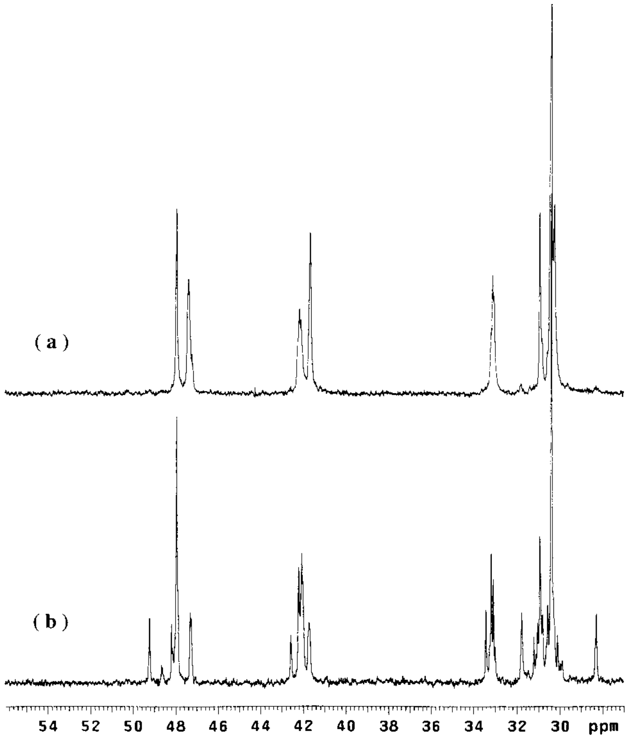

Figure 6. ^{13}C NMR spectra of P(E-*co*-N)s with approximately 46 mol % norbornene produced by (a) [Me$_2$Si(Me$_4$Cp)(N^{t}Bu)]TiCl$_2$ (**1**, entry 7) and (b) *rac*-[Et(Ind)$_2$]ZrCl$_2$ (**5**, entry 47).

more than 46 mol % of the comonomer into the polymer chain with these CpA catalysts, suggesting that these CpA catalysts might be good candidates for producing alternating microstructures.

Poly(ethylene-*co*-norbornene) Microstructure. To date, analyses of the ^{13}C NMR spectra of P(E-*co*-N) are limited to general assignments of the ordering of methylenes and methynes. Previous studies of norbornene transition metal complexes and norbornene insertion into metal−carbon bonds have shown shown that the exo face is more reactive than the endo face, due to electronic and steric effects. In a study of hydrooligomerization of norbornene using chiral and achiral zirconocenes, Arndt and co-workers[39,40] were able to identify the resulting dimers and trimers by ^{13}C NMR. By comparison with alkylnorbornanes,[48−50] they assigned an exo-(exo,exo)-exo conformation as predominant for the hydrotrimers.

Roth and co-workers[51] were among the first to publish ^{13}C NMR spectroscopic analyses of P(E-*co*-N), and in their study they reported general assignments for the methylene and methyne chemical shifts. The gross ordering of methylenes and methynes was later modifed by Kaminsky,[15,52] by Fink and co-workers,[26,27,53] and by MacKnight.[34] Bergström and co-workers recently confirmed by COSY ^{1}H NMR that the exo face is enchained in the copolymer.[54]

The spectrum and structure of a low norbornene content P(E-*co*-N) are shown in Figure 5. One can utilize the ^{13}C NMR assignments to calculate the mole percent norbornene incorporation by comparing either the C$_4$ peak at 33 ppm or the average of C$_1$ and C$_2$ peaks at 41−48 ppm to the sum of the methylene peaks centered around 30 ppm. The two methods are shown in eqs 1 and 2, respectively,

$$\frac{100(I_1 + I_2)}{2I_{\mathrm{CH_2}}} = \%\ \mathrm{N} \tag{1}$$

$$\frac{200I_4}{I_{\mathrm{CH_2}}} = \%\ \mathrm{N} \tag{2}$$

where I_1 is the observed intensity for C$_1$, I_2 is the observed intensity of C$_2$, I_4 is the observed intensity of C$_4$, and $I_{\mathrm{CH_2}}$ is the observed intensity of C$_3$ and chain CH$_2$'s. An equation analogous to eq 1 was recently used by Bergström et al.[54] To accurately calculate the mole percent incorporation according to eq 1, which compares methynes to methylenes, long delays must be employed to compensate for different relaxation times. However, in our studies we have found eq 2 to be more useful since it compares only methylene resonances. Comparison of spectra obtained using relaxation delays of 0 and 10 s for individual copolymers confirmed that the incorporation values obtained using eq 2 under both conditions were within ±1 mol %.

At high levels of norbornene incorporation, it is apparent that CpA-derived P(E-*co*-N)s have different microstructures than the zirconocene-derived P(E-*co*-N)s. Figure 6 demonstrates this for two copolymers of approximately the same norbornene composition (46% N), one which was produced by Me$_2$Si(Me$_4$Cp)(N^{t}Bu)]TiCl$_2$ (**1**) and the other which was produced by *rac*-[Et(Ind)$_2$]ZrCl$_2$ (**5**). Catalyst **5** clearly favors the formation of what appear to be consecutive norbornene sequences,[26,34] which appear as sharp peaks at 28.3, 31.8, 33.4, 42.4, 48.2, 48.6, and 49.2 ppm.[54] The ability to produce longer norbornene sequences is likely a consequence of this catalyst's higher rate of norbornene homopolymerization.

Ethylene/norbornene copolymers with more than 5 mol % norbornene incorporation show splitting of the methylene and methyne regions as a result of sequence differentiation. In the methylene region of the ^{13}C NMR spectra of P(E-*co*-N)s produced by **1**, we can track the disappearance of the polyethylene S$_{\delta\delta}$ resonance and the growth of the C$_3$, C$_\alpha$, and C$_\beta$ resonances P(E-*co*-N) with increasing norbornene content (Figure 7).

Figure 8 illustrates similar trends in the methyne region for the same series of P(E-*co*-N)s produced by catalyst **1**. As norbornene incorporation increases, there is a growth of the peaks at 47.9, 47.4, 42.2, and 42.0 ppm and a corresponding decrease in the intensity of the peaks at 47.2 and 41.7 ppm. Moreover, the intensity ratio of the peaks at 47.9 and 47.4 ppm remains virtually constant as more norbornene is incorporated

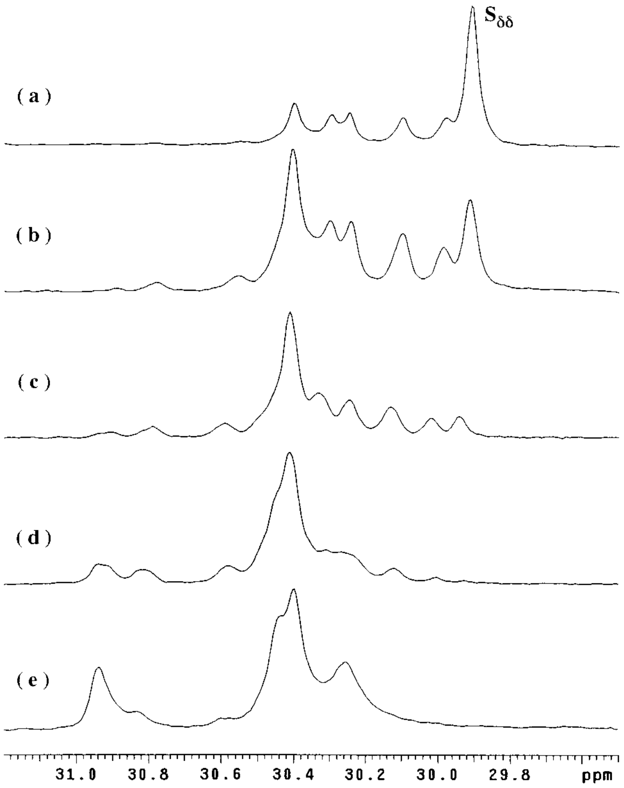

Figure 7. Methylene region of P(E-*co*-N)s produced by **1**: (a) 12% N (entry 2), (b) 22% N (entry 3), (c) 30% N (entry 4), (d) 40% N (entry 6), (e) 49% N (entry 7).

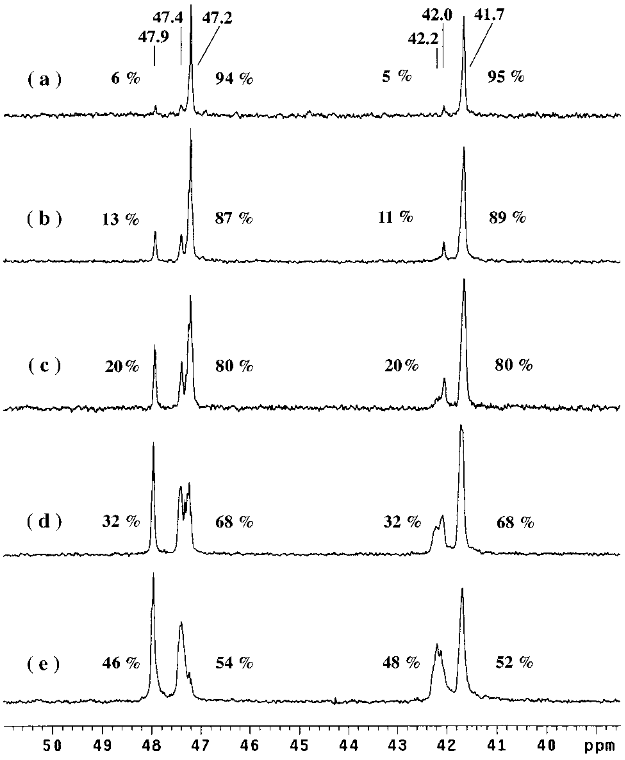

Figure 8. Methyne region of P(E-*co*-N)s produced by **1**: (a) 12% N (entry 2), (b) 22% N (entry 3), (c) 30% N (entry 4), (d) 40% N (entry 6), (e) 46% N (entry 7). The percentages listed beside each peak(s) are equivalent to the intensity of the peak(s) normalized to the total intensity of the specific methyne region.

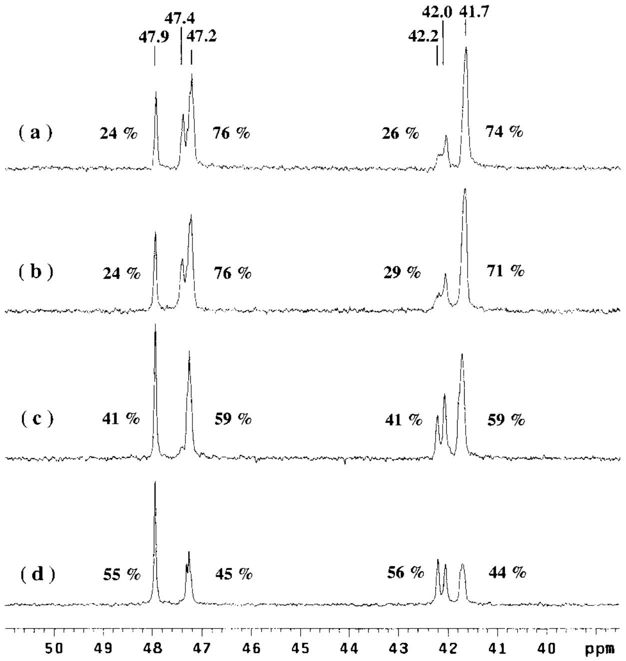

Figure 9. Methyne region of 34 mol % N P(E-*co*-N)s produced by different CpA catalysts: (a) [Me$_2$Si(Me$_4$Cp)(N^{t}Bu)]TiCl$_2$ (**1**, entry 5), (b) [Me$_2$Si(2,4-Me$_2$Cp)(N^{t}Bu)]TiCl$_2$ (**2**, entry 8), (c) [Me$_2$Si(3-^{t}BuCp)(N^{t}Bu)]TiCl$_2$ (**3**, entry 9), and (d) [Me$_2$Si(Ind)-(N^{t}Bu)]TiCl$_2$ (**4**, entry 10). The percentages listed beside each peak are equivalent to the intensity of the peak relative to the total intensity of the specific methyne region.

into the copolymer. It is also evident from Figure 8 that C$_1$ and C$_2$ are equally sensitive to the local monomer sequence, since the intensity ratio for the peak at 47.9 ppm vs the peaks centered at 47.4 ppm and the intensity ratio for the peaks centered at 42.2 ppm vs the peak at 41.7 ppm are virtually identical.

Our examinations of the ^{13}C NMR spectra of CpA-derived P(E-*co*-N)s revealed that formation of NN or NNN sequences was possible only at very low E/N feed ratios. While all the copolymers exhibited peaks at 47.9 and 47.4 ppm in their ^{13}C NMR spectra, resonances higher than 48 ppm were seen in a very low intensity for only two copolymers (see Supporting Information) which were produced by catalysts **3** and **4**, respectively, at low feed ratios (E/N $\leq$ 0.09). In sample 6, which was produced by **1** from a feed ratio of 0.05, we are able to detect minor resonances at 25.9 and 29.4 ppm of approximately 2% the intensity of the total methylene signals. These peaks are evident in the ^{13}C NMR spectra of a 43% N copolymer produced by **3** and in other high norbornene content P(E-*co*-N)s in the literature.[19,34,53] No resonances could be detected in the 36−40 ppm range where the C$_2$ carbons of norbornene hydrodimers and trimers are found. In general, the absence of resonances corresponding to NN sequences is consistent with very low r_2 values for the CpA catalysts and indicates a tendency for these catalysts to produce alternating copolymers.

The ratio of the methyne resonances also depends strongly on the geometry of the CpA catalyst. Figure 9 shows four copolymers containing approximately 34 mol % norbornene, and one can see that the peak intensities for C$_1$ (47.2−47.9 ppm) and C$_2$ (41.7−42.2 ppm) vary from copolymer to copolymer. The two copolymers produced by methylcyclopentadienyl-based catalysts **1** and **2** have identical splitting for the C$_2$ peak centered at 42.2 ppm and the C$_1$ peak centered at 47.4 ppm, and their relative peak intensities are approximately the same (25:75). Catalysts **3** and **4**, on the other hand, give

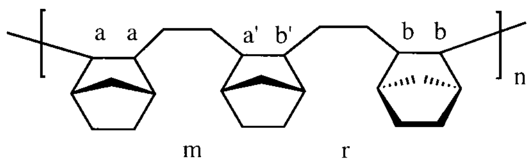

Figure 10. The meso and rac NEN sequences in P(E-*co*-N).

copolymers with quite different microstuctures, as the C_1 region is simplified to only two sharp resonances and the C_2 region shows three distinct resonances. In addition, the intensity ratios of the peaks at 47.9 ppm vs 47.4 ppm are higher for these two copolymers (41:59 and 55:45, respectively). While there remains some ambiguity in the chemical shift assignments (vide infra), the differences in the NMR spectra in Figure 9 are likely the consequence of differing tacticities in the copolymers.

One common method of estimating ^{13}C NMR chemical shifts for copolymers is to use the empirically derived additive relationships of Grant and Paul[55] and of Lindeman and Adams;[56] however, these relationships work well only for linear and slightly branched polymer systems, and they are not considered useful for differentiating peaks within 1 ppm of each other.[57] For highly branched poly(ethylene-*co*-cyclopentene), Kaminsky and Spiehl[42] compared experimentally assigned shifts with shifts calculated according to Grant and Paul and found that while the method was accurate for some kinds of carbon atoms, it gave errors as high as ±4 ppm for other carbons. As such, spectroscopy of molecular models is often necessary to explicitly assign the identity of each sequence. Presently no such models for poly(ethylene-*co*-norbornene) sequences have been reported in the literature.

More definitive conclusions are difficult to draw given the ambiguities in chemical shift assignments that have appeared in the literature for the methyne region (40−50 ppm).[17,19,26,33,34,53] For example, the resonances at 47.9 and 47.4 ppm have previously been assigned as the NENEN and NENEE signals, respectively.[17] These assignments seem inconsistent with the results shown in Figure 8, which show that these resonances increase equally with increasing norbornene incorporation. At close to 50% incorporation, the copolymer should be almost completely alternating in the absence of NN sequences. In the absence of tacticity effects, the ^{13}C NMR spectrum of a perfectly alternating ethylene−norbornene copolymer should simplify to five resonances. Polymers approaching this degree of regularity have been reported by Cherdron, Harrington, and Fink;[19,24,26] the spectrum in Figure 8e is more complex.

On the basis of the influence of increasing norbornene content in the copolymer on the methyne microstructure, we propose that the C_1 region contains resonances that can be partially attributed to the diastereosequences (*meso*- and *rac*-triad) sequences shown in Figure 10. It is known[58,59] that one can distinguish *meso*- and *rac*-PEP sequences in the ^{13}C NMR spectrum of poly(ethylene-*co*-propylene). It is therefore not unreasonable to assume that the tertiary carbons C_1 and C_2 of P(E-*co*-N) should display similar sensitivity to a local stereochemical environment.

From the spectra of various copolymers derived from **1** (Figure 8), it is clear that the ratio of the peaks at 47.9 and 47.4 ppm is constant with rising norbornene content. This is also true for catalyst **2**, as the ratio of these two peaks is constant for copolymers with norbornene levels between 10 and 40%. The attribution of these resonances to diastereosequences is consistent with the invariance of the ratio of these resonances to norbornene composition[60] and with the differences observed in the ratio of these resonances for the chiral catalysts **3** and **4** (Figure 9). The degree of stereoregularity of these polymers would appear to be inferior to that reported by Cherdron, Harrington, and Fink,[19,24,26] but more detailed analysis of the P(E-*co*-N) spectra is needed before the microstructure of these copolymers can be completely assigned.[26,34,55]

Conclusions

These studies show that CpA catalysts, because of their open active site, can insert norbornene effectively into a polyethylene chain. However, norbornene homopolymerization appears to be much slower for CpA complexes than for zirconocenes; correspondingly, the CpA-derived copolymers have few NN sequences. Analysis of the ^{13}C NMR spectra of P(E-*co*-N)s produced by the CpA catalysts gives us new information about the microstructure of these copolymers. The combination of low homopropagation to cross-propagation rate ratios (r_1 and r_2) for CpA catalysts and the conspicuous lack of norbornene dimers and trimers in the ^{13}C NMR spectra lead us to the conclusion that these catalysts have an increased tendency toward alternation relative to most zirconocenes. At high norbornene contents (≥40%), P(E-*co*-N)s produced by CpA catalysts exhibit ^{13}C NMR spectra that contain two large C_1 resonances at 47.9 and 47.4 ppm in ratios that are dependent on catalyst structure. These resonances are likely attributable to meso and rac NEN sequences (rather than EENEE or NENEE sequences, as previously proposed) although further studies are warranted to provide firm assignments of the NMR spectra of these polymers.

Experimental Section

General Conditions. All experiments involving air-sensitive compounds were performed under nitrogen in a Vacuum Atmospheres drybox or under argon using standard Schlenk line techniques. Hydrocarbon solvents, diethyl ether, tetrahydrofuran, benzene-d_6, tetrahydrofuran-d_8, and toluene-d_8 were distilled from sodium/benzophenone ketyl. Methylene chloride, chloroform, chloroform-*d*, and dimethylformamide were distilled from calcium hydride. Deuterated solvents were obtained from Cambridge Isotopes Labs.

Butyllithium, dimethyldichlorosilane, isopropylmagnesium chloride, and lead(II) chloride were obtained from Aldrich and used as received. Indene (Wiley) was dried over 3 Å molecular sieves and distilled. *tert*-Butylamine was obtained from Aldrich and distilled from calcium hydride. $[Me_2Si(Me_4Cp)(N^tBu)]Mg_2Cl_2(THF)_2$,[4] $TiCl_3(THF)_3$,[61] and $Ti(NMe_2)_4$[62] were prepared according to literature procedures. $[Me_2Si(Ind)(N^tBu)]TiCl_2$[63] was prepared by amine elimination.[9] *rac*-$[Et(Ind)_2]ZrCl_2$ (**5**) and Cp_2ZrCl_2 (**7**) were purchased from Strem, and $[Me_2C(Flu)(Cp)]ZrCl_2$ (**6**) was synthesized according to a literature procedure.[45]

Ethylene (Matheson) and toluene (Aldrich) were passed over activated alumina and Q-5 catalyst (Engelhard) to remove oxygen and water. Norbornene (Aldrich) was dried over calcium hydride for 24−48 h at 60 °C and then vacuum transferred. The purified norbornene was dissolved in a minimal amount of toluene, and the composition of this stock solution was determined by GC.

^1H NMR spectra were recorded on Varian XL-400 spectrometer and were referenced relative to TMS while ^{13}C NMR spectra were recorded at 75 MHz on a Varian Unity-300 NMR spectrometer. Elemental Analyses were performed by Desert Analytics.

Norbornene Homopolymerizations. In a typical experiment, a 100 mL Schlenk tube was charged with MAO (118 mg) in a glovebox, and a stock solution of norbornene in toluene was added. An additional portion of toluene was added to bring the volume to 49 mL, and a 1 mL aliquot (1 μmol) of a catalyst stock solution in toluene was added to initiate the polymerization. The vessel was brought out of the glovebox and placed under argon atmosphere on a vacuum/argon manifold to stir at room temperature. Polymerizations at 80 °C were heated with an oil bath, and an H_2O coldfinger was placed in the Schlenk tube to minimize evaporation. Reactions were later quenched with MeOH, and the reaction contents were poured into excess acidic MeOH to precipitate the homopolymer.

Ethylene/Norbornene Copolymerizations. In a typical experiment, a 6 oz. glass pressure vessel (Andrews Glass Co.) was charged with a stock solution of norbornene in toluene and a Teflon stir bar, and toluene was then added to bring the volume to 80 mL. The glass vessel was capped and sealed with a metal reactor head, which was equipped with pressure gauge, relief valve, and a Swagelock “quick connect”. This was pressurized with ethylene with stirring (900 rpm) for 20 min at 40 °C using a thermostated (±1 °C) water bath. Meanwhile, a 1 mL aliquot (2 μmol) of a catalyst stock solution was treated with a 19 mL solution of solid MAO (236 mg, 4 mmol, Akzo type 4A) in toluene. After 20 min equilibration time, the catalyst solution was loaded into an injector tube, and the polymerization was initiated by quickly venting the reactor to a reduced pressure and then injecting the catalyst solution with an ethylene back pressure. Polymerizations were terminated by venting ethylene and then injecting MeOH (10 mL). Polymers were precipitated by pouring the reactor contents into acidic MeOH (400 mL) and stirring overnight. Finally, the polymer was filtered, washed with MeOH, and dried at 40−50 °C in a vacuum oven.

Determination of [Ethylene]. Ethylene concentrations in toluene can be calculated according to the Henry−Gesetz expression[64]

$$[\mathrm{E}] = P_{\mathrm{E}} H_0 \exp\left(\frac{\Delta H_{\mathrm{L}}}{RT}\right) \tag{3}$$

where [E] is the ethylene concentration (mol/L), P_{E} is the ethylene pressure (bar), H_0 is the Henry coefficient, ΔH_{L} is the enthalpy of solvation for ethylene, R is the universal gas constant, and T is the solution temperature (K). For toluene, $H_0 = 0.00175$ mol/(L bar) and $\Delta H_{\mathrm{L}} = 10\,742$ W s/mol.[64] These calculated ethylene concentrations agree well with solubility measurements performed by Konobeev and Lyapin.[65]

To obtain ethylene concentrations for our system, an experiment was conducted using a digitally monitored ethylene reservoir which provided ethylene of a specific pressure on demand to a stirred PARR reactor. Toluene ($V_{\mathrm{solution}} = 100$ mL) was injected into the reactor with an argon back pressure and equilibrated at 40 °C. The solution was marginally degassed of argon without stirring by passing ethylene (15 psig) over the headspace. To initiate the dissolution experiment, mechanical stirring was activated, and the initial pressure of the reservoir was noted. The solution was stirred for 20−30 min to ensure complete saturation, and then the final head and reservoir pressures were noted. Stirring was stopped, and the head pressure was increased to 30 psig. The saturation experiment was repeated at this pressure and at subsequent pressures of 45, 60, 75, and 90 psig. The data collected were used to obtain the number of moles dissolved (Δn) at each pressure according to the ideal gas law:

$$\Delta PV = \Delta nRT \tag{4}$$

where ΔP is the total change in reservoir pressure for a given head pressure, V is the volume of the reservoir system (0.446 L), R is the gas constant (1.206 L psi/(mol K)), and T is the reservoir temperature (299 K). The concentration is thus defined as $\Delta n/V_{\mathrm{solution}}$. A plot of $[\mathrm{E}]_{\mathrm{observed}}$ and $[\mathrm{E}]_{\mathrm{calculated}}$ vs the final head pressure (see Supporting Information) shows identical linear dependences for these observed ethylene concentrations and those calculated according to the Henry−Gesetz expression. The intercept for $[\mathrm{E}]_{\mathrm{observed}}$ is less than 0 M due to residual argon (ca. 1 bar) in solution.

Polymer Characterizations. ^{13}C NMR spectra of poly(ethylene-*co*-norbornene) samples (150−200 mg) were obtained in a 9:1 mixture of *o*-$Cl_2-C_6H_4$ and C_6D_6 (3.0 mL) at 100 °C. A spectral width of 200 ppm, a pulse width of 7.0 ms, an acquistion time of 1.0 s, and no relaxation delay were used for an average of 320 transients for each spectrum. Chemical shifts were referenced to *o*-$Cl_2-C_6H_4$ (130.4 ppm).

Glass transition temperatures were measured on a Perkin-Elmer DSC 7. For measurements of glass transition temperatures, melt pressed samples were prepared by heating to 180−200 °C and then crash cooling in liquid nitrogen to erase the thermal history. Each sample was then heated from −40 to 300 °C and then cooled to −40 °C (20 °C/min). The scan was repeated, and data are reported for this second scan. To analyze for crystallinity, samples were annealed at 180 °C for 8 h and then slowly cooled at a rate of 2 °C/min to room temperature. A heating scan was run from 25 to 350 °C at a rate of 20 °C/min. No melting transitions were seen for sample 6, 7, 10, or 12.

GPC measurements were conducted by Polymer Laboratories on 2 mg/mL filtered samples using a PL-GPC210 system with a Mixed-B 3 x (PLgel 10 μm) column set at 160 °C in 1,2,4-trichlorobenzene. The system was calibrated using polystyrene standards. Two methods of detection were used versus polystyrene standards: (a) DRI and (b) viscometry (Viscotek 210R). The DRI response for P(E-*co*-N)s varied significantly from one sample to another and generally were very small, indicating very low dn/dc. As a result, light scattering detectors did not show a significant response. Samples with less than 34 mol % norbornene gave negative DRI responses while samples with greater than 34 mol % norbornene gave positive DRI responses. Viscometry, while sensitive to both concentration and specific viscosity (which is influenced by composition), was the only means of assessing a large data set. The polydispersities reported in Table 2 tend to be lower than expected since the viscometer has poor sensitivity in the low-M_{w} region.

[$Me_2Si(Me_4Cp)(N^tBu)]TiCl_2$ (1). A mixture of [$(Me_4Cp)SiMe_2N^tBu]Mg_2Cl_2(THF)_2$ (2.00 g, 3.90 mmol) and $TiCl_3(THF)_3$ (1.46 g, 3.94 mmol) was treated at −78 °C with THF (60 mL) with shaking. The light blue suspension was warmed to room temperature, darkening quickly to a deep red solution. After stirring 10 min, $PbCl_2$ (0.548 g, 1.97 mmol) was added as a solid, and lead precipitated immediately. THF was removed in vacuo after 8 h, and the residue was extracted with pentane (2 × 30 mL). Concentrating to 30 mL and cooling to −78 °C for 2 h gave a yellow microcrystalline solid (**1**). Yield: 0.767 g (53.4%). ^{1}H NMR (C_6D_6): δ 2.00 (s, 6H, Cp−CH_3), 1.99 (s, 6H, Cp−CH_3), 1.42 (s, 9 H, NC(CH_3)$_3$, 0.43 (s, 6H, Si(CH_3)$_2$). ^{13}C NMR (C_6D_6): δ 140.8, 138.1, 121.6, 62.4, 32.9, 16.4, 13.3, 5.6. Anal. Calcd for $C_{15}H_{27}Cl_2NSiTi$: C, 48.92; H, 7.39; N, 3.80. Found: C, 49.34; H, 7.57; N, 3.78.

1,3-Me_2CpH_2.[66] MeMgBr (80.0 mL, 3.0 M in Et_2O) was treated at 0 °C with THF (80 mL), giving a thick suspension. This was treated dropwise over a period of 1.5 h with 3-methyl-2-cyclopentenone (11.5 g, 120 mmol). After stirring an additional 3.5 h at 0 °C, volatiles were removed in vacuo. Addition of Et_2O (100 mL) at 0 °C followed by slow addition of saturated NH_4Cl (100 mL) gave a clear supernatant and a white gelatinous mass. The supernatant was decanted, and the solids were washed with Et_2O (2 × 25 mL). The combined organics were washed with H_2O (50 mL), dried over $MgSO_4$, filtered, and then concentrated in vacuo to give a yellow-orange oil. Vacuum transfer of this oil gave a clear, colorless liquid, which was subsequently treated with p-TsOH (0.029 g) at 0 °C and stirred overnight at 0 °C. The oil was then washed several times with H_2O, dried over $MgSO_4$, and filtered. Vacuum transfer of this yellow oil gave a clear, colorless liquid, which was used immediately for deprotonation (vide supra). ^{1}H NMR ($CDCl_3$): δ 5.98 (s, 1H, vinylic Cp−H), 5.77 (s, 1H, vinylic Cp−H), 2.82 (d, 2H, allylic Cp−H), 2.03 (s, 3H, Cp−CH_3), 1.93 (s, 3H, Cp−CH_3).

(1,3-Me$_2$CpH)Li. A solution of 1,3-Me$_2$CpH$_2$ (assuming 120 mmol) in Et$_2$O (100 mL) was cooled to −78 °C and treated dropwise with BuLi (48 mL, 2.5 M in hexane) to give a yellow suspension. After warming to room temperature and stirring 6 h, the suspension was filtered. The white solid was washed with hexane (2 × 50 mL) and dried in vacuo. Yield: 3.898 g (38.9 mmol, 32.5% based on 3-methyl-2-cyclopentenone).

Me$_2$Si(2,4-Me$_2$CpH)Cl. A solution of Me$_2$SiCl$_2$ (83.7 g, 648 mmol) in THF (50 mL) was cooled to 0 °C and treated dropwise over 45 min with a solution of (1,3-Me$_2$CpH)Li (48 mL, 2.5 M in hexane) in THF (90 mL). The resulting yellow solution was warmed to room temperature and stirred overnight. Volatiles were then removed in vacuo, and the yellow paste was extracted with hexane (3 × 10 mL). The yellow filtrate was concentrated in vacuo and then purified by vacuum distillation (bp 68 °C/12 mmHg). Yield: 4.854 g (26.0 mmol, 68.8%). ^{1}H NMR (CDCl$_3$, mixture of isomers): δ 6.14, 6.08, 5.83 (s, 2H, vinylic Cp−H), 3.30, 3.05 (s, 1 H, allylic Cp−H), 2.13, 2.10, 2.07, 1.99 (s, 6H, Cp−CH_3), 0.59, 0.39, 0.18 (s, 6H, Si(CH_3)$_2$).

Me$_2$Si(2,4-Me$_2$CpH)(NH^{t}Bu). A solution of Me$_2$Si(2,4-Me$_2$CpH)Cl (4.85 g, 26.0 mmol) in THF (60 mL) was treated with *tert*-butylamine (5.70 g, 78.0 mmol) via a syringe. The resulting suspension was stirred overnight. Volatiles were removed in vacuo, and the pale yellow paste was extracted with pentane (3 × 10 mL). The yellow filtrate was concentrated in vacuo and then purified by vacuum distillation (bp 80 °C/200 mTorr). Yield: 5.441 g (21.7 mmol, 68.1%). ^{1}H NMR (CDCl$_3$): δ 6.03 (s, 1H, vinylic Cp−H), 5.85 (s, 1H, vinylic Cp−H), 3.09 (s, 1H, allylic Cp−H), 2.95 (s, 1H, allylic Cp−H) 6.63 (m, 3H, vinylic Cp−H), 3.37 (s, 1H, Cp−H), 3.02 (s, 1H, allylic Cp−H), 2.11, 2.08, 2.06, 1.98 (s, 6H, Cp(CH_3)$_2$), 1.18, 1.12 (s, 9H, NC(CH_3)$_3$), 0.55 (s, 1H, NH) 0.21, 0.10, 0.01, −0.10 (s, 3H, Si(CH_3)$_2$).

[Me$_2$Si(2,4-Me$_2$Cp)(N^{t}Bu)TiCl$_2$ (2). A solution of Me$_2$Si(2,4-Me$_2$CpH)(NH^{t}Bu) (0.524 g, 2.34 mmol) and Ti(NMe$_2$)$_4$ (0.549 g, 2.34 mmol) in toluene (10 mL) was heated to reflux for 4 days under argon flow [Note: for complete conversion, it is important to maintain a good flow by purging the apparatus continually to an oil bubbler.] The dark red-brown solution was concentrated in vacuo to a thick red oil. ^{1}H NMR (C$_6$D$_6$): δ 5.72 (d, 1H, Cp−H), 5.66 (d, 1H, Cp−H), 3.08 (s, 6H, N(CH_3)$_2$), 2.85 (s, 6H, N(CH_3)$_2$), 2.09 (s, 3H, C$_p$CH_3), 2.05 (s, 3H, C$_p$CH_3), 1.33 (s, 9H, NC(CH_3)$_3$), 0.56 (s, 3H, Si(CH_3)$_2$), 0.52 (s, 3H, Si(CH_3)$_2$).

The red oil was dissolved in CH$_2$Cl$_2$ (10 mL), and then Me$_3$SiCl (0.32 mL, 2.5 mmol) was added via a syringe. Stirring overnight followed by concentration in vacuo gave a red oil. Pentane (15 mL) was added at −78 °C, giving rise to a yellow-brown precipitate. This was warmed to room temperature and filtered. Extraction of this solid with toluene (3 × 10 mL) at 50 °C gave a dark brown tar and a yellow extract. The combined pentane and toluene extracts were concentrated in vacuo to 10 mL and slowly cooled to −20 °C and then to −78 °C. The resulting yellow crystals were washed with cold pentane (2 × 5 mL) and dried in vacuo. Yield: 0.372 g (1.09 mmol, 46.7%). ^{1}H NMR (CDCl$_3$): δ 6.62 (d, 1H, Cp−H), 6.07 (d, 1H, Cp−H), 2.36 (s, 3H, C$_p$CH_3), 2.21 (s, 3H, C$_p$CH_3), 1.45 (s, 9H, NC(CH_3)$_3$), 0.68 (s, 3H, Si(CH_3)$_2$), 0.56 (s, 3H, Si(CH_3)$_2$). ^{13}C NMR (CDCl$_3$): δ 142.9, 139.9, 128.5, 127.3, 107.7, 63.2, 32.3, 18.2, 16.4, 3.03, 1.05. Anal. Calcd for C$_{13}$H$_{23}$Cl$_2$NSiTi: C, 45.89; H, 6.83; N, 4.12. Found: C, 46.09; H, 6.91; N, 4.34.

^{t}BuCpH$_2$.[67] A solution of 2-bromo-2-methylpropane (23.7 g, 173.3 mmol) in THF (90 mL) was heated to reflux, and then sodium cyclopentadienide (93.7 mL, 2.0 M in THF) was added dropwise over 1 h. The resulting dark red suspension was refluxed overnight and then poured into 100 mL of saturated NH$_4$Cl. The organic layer was separated, and the aqueous layer was washed with Et$_2$O (3 × 25 mL). The combined organics were washed with 100 mL of saturated NaCl and then dried over MgSO$_4$. After filtration, volatiles were stripped off in vacuo, leaving a yellow oil. Yield: 12.411 g (102 mmol, 54.4%). ^{1}H NMR (CDCl$_3$): δ 5.98−6.63 (m, 3H, vinylic Cp−H), 2.95 (s, 2H, allylic Cp−H), 1.19 (s, 9H, C(CH_3)$_3$).

Me$_2$Si(3-^{t}BuCpH)Cl.[68] A solution of ^{t}BuCpH$_2$ (6.00 g, 49.2 mmol) in THF (100 mL) was cooled to −78 °C and then treated dropwise with butyllithium (20.0 mL, 2.5 M in hexanes). The solution was warmed to room temperature and stirred overnight. This was then added dropwise to a solution of Me$_2$SiCl$_2$ (88.8 mL, 738 mmol) in THF (50 mL) at −78 °C. The solution was warmed to room temperature and stirred for several hours. Volatiles were removed in vacuo, and the resulting yellow paste was extracted 4 × 10 mL pentane. Concentrating the filtrate in vacuo and distilling (bp 80 °C/130 mTorr) gave a yellow oil as the main fraction. Yield: 6.83 g (31.8 mmol, 64.7%). ^{1}H NMR (CDCl$_3$): δ 6.08−7.04 (m, 3H, vinylic Cp−H), 3.50 (s, 1H, allylic Cp−H), 3.11 (d, 1H, allylic Cp−H), 1.20 (s, 9H, C(CH_3)$_3$), 0.58 (s, 3H, Si(CH_3)$_2$), 0.57 (s, 3H, Si(CH_3)$_2$), 0.27 (s, 3H, Si(CH_3)$_2$), 0.23 (s, 3H, Si(CH_3)$_2$).

Me$_2$Si(3-^{t}BuCpH)(NH^{t}Bu).[68] A solution of Me$_2$Si(3-^{t}BuCpH)Cl (6.83 g, 31.8 mmol) in THF (60 mL) was treated with *tert*-butylamine (6.99 g, 95.5 mmol) via a syringe. The resulting suspension was stirred overnight. Volatiles were removed in vacuo, and the pale yellow paste was extracted with pentane (1 × 25 mL, 2 × 10 mL). Concentrating the extract in vacuo and distilling (bp 52−58 °C/320 mTorr) gave a yellow oil as the main fraction. Yield: 5.441 g (21.7 mmol, 68.1%). ^{1}H NMR (CDCl$_3$): δ 6.08−6.63 (m, 3H, vinylic Cp−H), 3.37 (s, 1H, Cp−H), 3.02 (s, 1H, allylic Cp−H), 1.20 (s, 9H, NC(CH_3)$_3$), 1.19 (s, 9H, C(CH_3)$_3$), −0.02 (s, 3H, Si(CH_3)$_2$), −0.05 (s, 3H, Si(CH_3)$_2$).

[Me$_2$Si(3-^{t}BuCp)(N^{t}Bu)]TiCl$_2$ (3).[68] A solution of Me$_2$Si(3-^{t}BuCpH)(NH^{t}Bu) (0.300 g, 1.19 mmol) and Ti(NMe$_2$)$_4$ (0.268 g, 1.19 mmol) in toluene (10 mL) was heated to reflux for 4 days under argon flow [Note: for complete conversion, it is important to maintain a good flow by purging the apparatus continually to an oil bubbler.] The red solution was concentrated in vacuo to a thick red oil, which crystallizes below room temperature. ^{1}H NMR (C$_6$D$_6$): δ 6.22 (q, 1H, Cp−H), 5.96 (t, 1H, Cp−H), 5.92 (t, 1H, Cp−H), 2.95 (s, 6H, N(CH_3)$_2$), 2.93 (s, 6H, N(CH_3)$_2$), 1.32 (s, 9H, NC(CH_3)$_3$), 1.22 (s, 9H, C(CH_3)$_3$), 0.57 (s, 3H, Si(CH_3)$_2$), 0.52 (s, 3H, Si(CH_3)$_2$).

The red oil was dissolved in CH$_2$Cl$_2$ (10 mL), and then Me$_3$SiCl (0.32 mL, 2.5 mmol) was added via a syringe. Stirring overnight followed by concentration in vacuo gave a red oil. Pentane (10 mL) was added, and the solution was quickly cooled to −78 °C. A yellow precipitate formed, which was isolated by filtration and washed with cold pentane (3 × 2 mL). Recrystallization from pentane (5 mL) at −50 °C gave yellow-brown crystals. Yield: 0.126 g (0.342 mmol, 28.7%). ^{1}H NMR (CDCl$_3$): δ 7.01 (m, 1H, Cp−H), 6.45 (m, 1H, Cp−H), 6.23 (m, 1H, Cp−H), 1.45 (s, 9H, NC(CH_3)$_3$), 1.36 (s, 9H, C(CH_3)$_3$), 0.60 (s, 3H, Si(CH_3)$_2$), 0.59 (s, 3H, Si(CH_3)$_2$). ^{13}C NMR (CDCl$_3$): δ 156.7, 127.7, 125.0, 120.6, 108.0, 64.0, 33.7, 32.2, 30.5, 0.4, −0.1. Anal. Calcd for C$_{15}$H$_{27}$Cl$_2$NSiTi: C, 48.92; H, 7.39; N, 3.80. Found: C, 48.76; H, 7.15; N, 4.01.

Acknowledgment. We gratefully acknowledge support from the NSF-NYI program (NSF-DMR 9258334-003) and the donors of the Petroleum Research Fund, administered by the American Chemical Society. We thank Polymer Laboratories for GPC analysis.

Supporting Information Available: Complete ethylene/norbornene copolymerization data and Fineman−Ross plots for catalysts **1**−**7**, Kelen−Tüdos plot for catalyst **1**, and ethylene solubility data. This material is available free of charge via the Internet at http://pubs.acs.org.

References and Notes

(1) Pannell, R. B.; Canich, J. A. M.; Hlatky, G. G. (Exxon) PCT Int. Appl. WO 94/00500, 1994.
(2) Canich, J. A. M. (Exxon) Eur. Pat. Appl. 0 420 436 A1, 1991.
(3) Canich, J. A. M. (Exxon) U.S. Patent 5,096,867, 1992.
(4) Stevens, J. C.; Timmers, F. J.; Wilson, D. R.; Schmidt, G. F.; Nickias, P. N.; Rosen, R. K.; Knight, G. W.; Lai, S.-y. (Dow) Eur. Pat. Appl. 0 416 815 A2, 1991.
(5) LaPointe, R. E.; Stevens, J. C.; Nickias, P. N.; McAdon, M. H. (Dow) Eur. Pat. Appl. 0 520 732 A1, 1992.
(6) Sernetz, F. G.; Muelhaupt, R.; Waymouth, R. M. *Macromol. Chem. Phys.* **1996**, *197*, 1071−83.
(7) Stevens, J. C. *Stud. Surf. Sci. Catal.* **1994**, *89*, 277−84.

(8) Swogger, K. W.; Lancaster, G. M. *Stud. Surf. Sci. Catal.* **1994**, *89*, 285−298.
(9) McKnight, A. L.; Masood, M. A.; Waymouth, R. M.; Straus, D. A. *Organometallics* **1997**, *16*, 2879−2885.
(10) Breslow, D. S. *Prog. Polym. Sci.* **1993**, *18*, 1141−1195.
(11) Sartori, G.; Ciampelli, F.; Cameli, N. *Chim. Ind.* **1963**, *45*, 1479.
(12) Sen, A.; Lai, T.-W. *Organometallics* **1982**, *1*, 415−417.
(13) Breunig, S.; Risse, W. *Makromol. Chem.* **1992**, *193*, 2915−2927.
(14) Kaminsky, W.; Bark, A.; Däke, I. *Stud. Surf. Sci. Catal.* **1990**, *56*, 425−438.
(15) Kaminsky, W.; Bark, A.; Arndt, M. *Makromol. Chem., Macromol. Symp.* **1991**, *47*, 83−93.
(16) Kaminsky, W.; Noll, A. *Polym. Bull.* **1993**, *31*, 175−182.
(17) Kaminsky, W.; Arndt, M.; Beulich, I. *Polym. Mater. Sci. Eng.* **1997**, *76*, 18−19.
(18) Goodall, B. L.; McIntosh, L. H.; Rhodes, L. F. *Macromol. Symp.* **1995**, *89*, 421−432.
(19) Cherdron, H.; Brekner, M.-J.; Osan, F. *Angew. Makromol. Chem.* **1994**, *223*, 121−133.
(20) Canich, J. A. M. (Exxon) PCT Int. Appl. WO 96/00244, 1996.
(21) Devore, D. D.; Crawford, L. H.; Stevens, J. C.; Timmers, F. J.; Mussell, R. D.; Wilson, D. R.; Rosen, R. K. (Dow) PCT Int. Appl. WO 95/00526, 1995.
(22) Harrington, B. A. (Exxon) PCT Int. Appl. WO 96/40806, 1996.
(23) Harrington, B. A.; Hlatkey, G. G.; Canich, J. A. M.; Merrill, N. A. (Exxon) U.S. Patent 5,635,573, 1997.
(24) Harrington, B. A.; Crowther, D. J. *J. Mol. Catal. A: Chem.* **1998**, *128*, 79−84.
(25) Ruchatz, D.; Fink, G. *Macromolecules* **1998**, *31*, 4669−4673.
(26) Ruchatz, D.; Fink, G. *Macromolecules* **1998**, *31*, 4674−4680.
(27) Ruchatz, D.; Fink, G. *Macromolecules* **1998**, *31*, 4681−4683.
(28) Ruchatz, D.; Fink, G. *Macromolecules* **1998**, *31*, 4684−4686.
(29) Herrmann, W. A.; Morawietz, M. J. A. *J. Organomet. Chem.* **1994**, *482*, 169−181.
(30) Carpenetti, D. W.; Kloppenburg, L.; Kupec, J.; Peterson, J. L. *Organometallics* **1996**, *15*, 1572−1581.
(31) Jordan, R. F.; Diamond, G. M.; Christopher, J. N.; Kim, I. *Polym. Prepr.* **1996**, *37*, 256.
(32) Luinstra, G. A.; Teuben, J. H. *J. Chem. Soc., Chem. Commun.* **1990**, 1470−1471.
(33) Bergström, C. H.; Vaananen, T. L. J.; Seppälä, J. V. *J. Appl. Polym. Sci.* **1997**, *63*, 1071−1076.
(34) Rische, T.; Waddon, A. J.; Dickinson, L. C.; MacKnight, W. J. *Macromolecules* **1998**, *31*, 1871−1874.
(35) Bergström, C. H.; Seppälä, J. V. *J. Appl. Polym. Sci.* **1997**, *63*, 1063−1070.
(36) Soga, K.; Uozumi, T.; Nakamura, S.; Toneri, T.; Teranishi, T.; Sano, T.; Arai, T.; Shiono, T. *Macromol. Chem. Phys.* **1996**, *197*, 4237−4251.
(37) Stevens, J. C. *Stud. Surf. Sci. Catal.* **1996**, *101*, 11−20.
(38) Kaminsky, W.; Engehausen, R.; Kopf, J. *Angew. Chem., Int. Ed. Engl.* **1995**, *34*, 2273−5.
(39) Arndt, M.; Engehausen, R.; Kaminsky, W.; Zoumis, K. *J. Mol. Catal. A: Chem.* **1995**, *101*, 171−8.
(40) Arndt, M.; Kaminsky, W. *Macromol. Symp.* **1995**, *97*, 225−46.
(41) Arndt, M.; Kaminsky, W. *Macromol. Symp.* **1995**, *95*, 167−83.
(42) Kaminsky, W.; Spiehl, R. *Makromol. Chem.* **1989**, *190*, 515−526.
(43) Kaminsky, W.; Noll, A. In *Ziegler Catalysis*; Fink, G., Muelhaupt, R., Brintzinger, H. H., Eds.; Springer: Berlin, Germany, 1995; pp 149−58.
(44) Kaminsky, W.; Külper, K.; Brintzinger, H. H.; Wild, F. R. W. P. *Angew. Chem., Int. Ed. Engl.* **1985**, *24*, 507−508.
(45) Ewen, J. A.; Jones, R. L.; Razavi, A.; Ferrara, J. D. *J. Am. Chem. Soc.* **1988**, *110*, 6255.
(46) Ewen, J. A.; Elder, M. J.; Jones, R. L.; Curtis, S.; Cheng, H. N. In *Catalytic Olefin Polymerization*; Keii, T., Soga, K., Eds.; Kodansha: Tokyo, 1990; pp 439−482.
(47) Kelen, T.; Tüdos, F. *J. Macromol. Sci.: Chem.* **1975**, *A9* (1), 1−27.
(48) Grutzner, J. B.; Jautelat, M.; Dence, J. B.; Smith, R. A.; Roberts, J. D. *J. Am. Chem. Soc.* **1970**, *92*, 7107−7120.
(49) Lippmaa, E.; Pehk, T.; Paasivirta, J.; Belikova, N.; Plate, A. *Organ. Magn. Reson.* **1970**, *2*, 581−604.
(50) Stothers, J. B.; Tan, C. T.; Teo, K. C. *Can. J. Chem.* **1973**, *51*, 2893−2901.
(51) Roth, H.; Meyer, U.; Koinzer, J.-P.; Wiegand, G. *Plaste Kautsch.* **1985**, *32*, 291−294.
(52) Kaminsky, W.; Arndt, M.; Bark, A. *Polym. Prepr.* **1990**, *32*, 467−468.
(53) Montag, P.; Ruchatz, D.; Fink, G. *Kautsch. Gummi Kunstst.* **1996**, *49*, 582−584, 586−588.
(54) Bergström, C. H.; Sperlich, B. R.; Ruotoistenmäki, J.; Seppälä, J. V. *J. Polym. Sci. A* **1998**, *36*, 1633−1638.
(55) Grant, D. M.; Paul, E. G. *J. Am. Chem. Soc.* **1964**, *86*, 2984−2990.
(56) Lindeman, L. P.; Adams, J. Q. *Anal. Chem.* **1971**, *43*, 1245−1252.
(57) Randall, J. C. *J. Macromol. Sci. C: Rev. Macromol. Chem. Phys.* **1989**, *29*, 201−317.
(58) Zetta, L.; Gatti, G.; Audisio, G. *Macromolecules* **1978**, *11*, 763−766.
(59) Tonelli, A. E. *Macromolecules* **1978**, *11*, 634−636.
(60) A referee has pointed out that there should be at least two methyne signals for rac and meso diastereosequences (a vs a′ and b vs b′ in Figure 10). This may be evident in the widths and splitting of the resonances observed in 47.4 and 47.9 ppm in Figures 8 and 9.
(61) Manzer, L. *Inorg. Synth.* **1982**, 135.
(62) Bradley, D. C.; Thomas, I. M. *J. Chem. Soc.* **1960**, 3857.
(63) Amor, F.; Okuda, J. *J. Organomet. Chem.* **1996**, *520*, 245.
(64) Krauss, V. W.; Gestrich, W. *CHEMTECH* **1977**, *6*, 513−516.
(65) Konobeev, B. I.; Lyapin, V. V. *Khim. Promst.* **1967**, *43*, 114−116.
(66) Reinmuth, A. Thesis, Universität Konstanz, 1992.
(67) Fischer, B.; Boersma, J.; van Koten, G.; Spek, A. L. *New J. Chem.* **1988**, *12*, 613−620.
(68) Okuda, J. *Chem. Ber.* **1990**, *123*, 1649.

MA981365V